Journal of Biomechanics 88 (2019) 4–11

Contents lists available at ScienceDirect

Journal of Biomechanics

journal homepage: www.elsevier.com/locate/jbiomech
www.JBiomech.com

A mathematical model to investigate the effects of intravenous fluid administration and fluid loss

Tilaï T. Rosalina [a,*], R. Arthur Bouwman [b,c,d], Marc R.H.M. van Sambeek [a,c], Frans N. van de Vosse [a], Peter H.M. Bovendeerd [a]

[a] Department of Biomedical Engineering, Eindhoven University of Technology, P.O. Box 513, 5600 MB Eindhoven, the Netherlands
[b] Department of Electrical Engineering, Eindhoven University of Technology, P.O. Box 513, 5600 MB Eindhoven, the Netherlands
[c] Catharina Hospital Eindhoven, Michelangololaan 2, 5623 EJ Eindhoven, the Netherlands
[d] Philips Research Eindhoven, High Tech Campus 34, Eindhoven, the Netherlands

ARTICLE INFO

Article history:
Accepted 1 March 2019

Keywords:
Fluid administration
Mathematical models
Transcapillary fluid exchange
Model assisted decision support

ABSTRACT

The optimal fluid administration protocol for critically ill perioperative patients is hard to estimate due to the lack of tools to directly measure the patient fluid status. This results in the suboptimal clinical outcome of interventions. Previously developed predictive mathematical models focus on describing the fluid exchange over time but they lack clinical applicability, since they do not allow prediction of clinically measurable indices. The aim of this study is to make a first step towards a model predictive clinical decision support system for fluid administration, by extending the current fluid exchange models with a regulated cardiovascular circulation, to allow prediction of these indices. The parameters of the model were tuned to correctly reproduce experimentally measured changes in arterial pressure and heart rate, observed during infusion of normal saline in healthy volunteers. With the resulting tuned model, a different experiment including blood loss and infusion could be reproduced as well. These results show the potential of using this model as a basis for a decision support tool in a clinical setting.

1. Introduction

Intravenous fluid infusion, to compensate for perioperative fluid loss due to bleeding, perspiration and evaporation, is a common procedure to maintain arterial blood pressure and thereby tissue perfusion. However, part of the administered fluid will shift to the interstitial space, causing edema buildup that may eventually compress tissue microvasculature, disturb tissue perfusion and could lead to organ failure. Especially in the critically ill, these 'fluid shifts' can be large and unpredictable, due to changes in endothelial permeability and hydrostatic and osmotic pressure (Holte et al., 2002; Brandstrup, 2006). The optimal protocol for fluid administration depends on the intra- and extravascular fluid status of the patient. This fluid status is not directly measurable, and it cannot be easily deduced from indirect measurements. Additionally there is a large inter-patient variability, which makes evidence-based predictions difficult. Hence, it remains difficult to estimate the amount of fluid needed to compensate perioperative fluid loss. A patient specific mathematical model might be used to assist in determining the optimal fluid protocol.

In literature various mathematical models have been presented that focus on fluid administration and (re-) distribution. Some models describe fluid exchange between intra- and extravascular spaces using Starling's law, based on hydrostatic and osmotic pressures (Chapple et al., 1993; Xie et al., 1995; Gyenge et al., 1999, 2003; Mazzoni et al., 1988; Carlson et al., 1996; Wolf and Watson, 1989; Wolf and Deland, 2011; Wolf, 2013). Other models use a more phenomenological volume kinetics approach (Hahn and Svensén, 1997; Svensén et al., 1999; Hahn, 2010, 2017). Since the first type of models are based on laws of physics and physiology, they provide a stronger basis to predict the internal condition and the clinically observed information of a perioperative patient.

However, previously published models of this type have a limited representation of the cardiovascular circulation and lack information on arterial pressure and heart rate. Since arterial pressure is one of the important clinically available measurements used to guide fluid administration, it is hard to apply these models clinically.

We aim to develop a decision support model that can eventually assist in fluid administration to critically ill patients based

* Corresponding author at: Eindhoven University of Technology, Department of Biomedical Engineering, P.O. Box 513, 5600 MB Eindhoven, the Netherlands.
E-mail address: t.t.rosalina@tue.nl (T.T. Rosalina).

https://doi.org/10.1016/j.jbiomech.2019.03.002
0021-9290/

on clinically available information such as arterial pressure and heart rate. In this study we extend a fluid exchange model (Xie et al., 1995) with a model of cardiovascular function (Jongen et al., 2016). Model parameters are partly taken from literature (Gyenge et al., 1999, 2003; Jongen et al., 2016), and partly determined from a fit to an experimental dataset of saline infusion (Watenpaugh et al., 1992). We evaluate our model by simulating another volunteer dataset of fluid administration in hypo- and normovolemia. Finally, we compare our model, with a regulated cardiovascular system, to the original fluid exchange model.

2. Methods

The model (Fig. 1) combines submodels of cardiovascular hemodynamics, cardiovascular regulation, fluid exchange, and renal function.

2.1. Submodel: fluid exchange

The fluid exchange model is taken from Xie et al. (1995). It consists of a vascular and an interstitial compartment. The vascular compartment consists of plasma (with volume V_{PL} in ml), red blood cells (V_{RBC} in ml) and proteins (with mass M_{PL} in g), where the volume occupied by the proteins is neglected. The ratio of red blood cells to plasma is given by the hematocrit (H_{ct}):

$$H_{ct} = \frac{V_{RBC}}{(V_{RBC} + V_{PL})} \cdot 100\%. \tag{1}$$

The concentration of proteins in the plasma (c_{PL} in $\frac{g}{ml}$) is calculated as:

$$c_{PL} = \frac{M_{PL}}{V_{PL}}. \tag{2}$$

The interstitial compartment consists of fluid, with volume V_I, and proteins, with mass M_I. A part of this volume, the excluded volume ($V_{I,ex}$), is not available as a solvent for protein. This volume includes other macromolecules such as collagen and fibrin (Xie et al., 1995). Therefore we distinguish between interstitial protein concentration (c_I), and available interstitial protein concentration (c_{IA}):

$$c_I = \frac{M_I}{V_I}, \qquad c_{IA} = \frac{M_I}{(V_I - V_{I,ex})}. \tag{3}$$

The exchange of fluid between compartments satisfies the mass balance:

$$\frac{dV_{PL}}{dt} = J_{intake} + J_{inf} - J_{V,TC} + J_{V,L} - J_U - J_{V,\,bleed} \tag{4}$$

$$\frac{dV_I}{dt} = J_{V,TC} - J_{V,L} - J_{ins}. \tag{5}$$

Here, J_{intake} is the basal intake in normovolemia in $\frac{ml}{s}$, J_{inf} is the infused fluid flow in $\frac{ml}{s}$, $J_{V,TC}$ is the transcapillary fluid flow in $\frac{ml}{s}$, $J_{V,L}$ is the lymph flow in $\frac{ml}{s}$, J_U is the urine flow in $\frac{ml}{s}$, $J_{V,\,bleed}$ is the plasma loss due to haemorrhage (J_{bleed}) in $\frac{ml}{s}$ and J_{ins} is the insensible fluid loss in $\frac{ml}{s}$. It holds that:

$$J_{V,bleed} = J_{bleed} \cdot (1 - H_{ct}). \tag{6}$$

The transcapillary fluid exchange ($J_{V,TC}$) is described by the Starling hypothesis:

$$J_{V,TC} = k_f \cdot [p_{cap} - p_I - \sigma(\pi_{cap} - \pi_I)]. \tag{7}$$

Here, k_f is the membrane permeability constant in $\frac{ml}{mmHg \cdot s}$, p in mmHg is the hydrostatic pressure, π in mmHg is the protein osmotic pressure, with subscripts *cap* for the capillaries and *I* for the interstitium, and σ [–] is the reflection coefficient. The capillary pressure is computed from the cardiovascular model, which will be described in Section 2.2. The interstitial pressure is calculated by empirical equations taken from Chapple et al. (1993), depending on the state of hydration:

$$p_I = \begin{cases} p_{I,N} + \frac{(V_I - V_{I,N})}{C_{under}} & V_I \leqslant V_{I,N} \\ p_{I,N} + \frac{(V_I - V_{I,N})}{C_{int}} & V_{I,N} < V_I < V_{I,over} \\ p_{I,over} + \frac{(V_I - V_{I,over})}{C_{over}} & V_I \geqslant V_{I,over} \end{cases}. \tag{8}$$

Here, $p_{I,N}$ is the interstitial pressure in normovolemia ($V_{I,N}$) and $p_{I,over}$ is the interstitial pressure at the threshold for hypervolemia ($V_{I,over}$). In the normovolemic range ($V_{I,N} < V_I < V_{I,over}$) p_I is determined by the normal interstitial compliance (C_{int}). The compliances

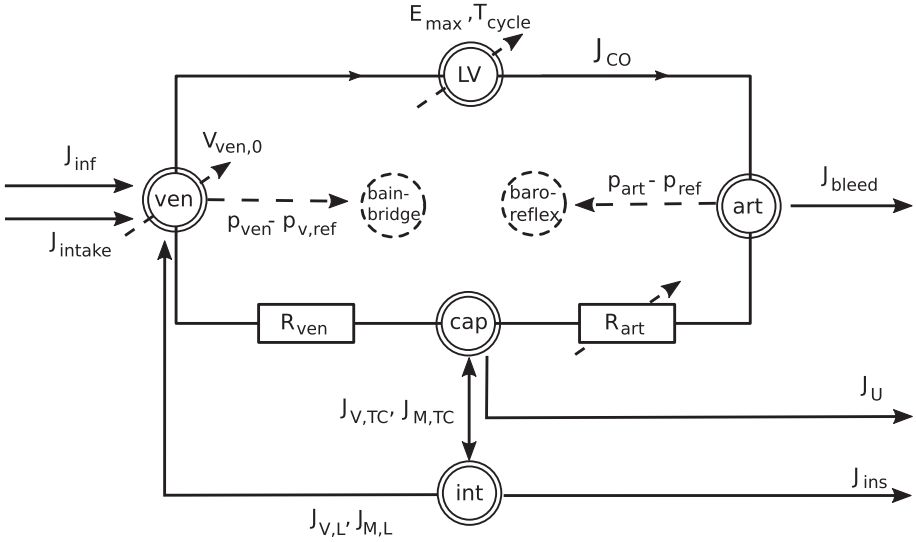

Fig. 1. Schematic overview of the mathematical model: the left ventricle (*LV*) generates a blood flow (J_{CO}) that passes through the arteries (*art*), capillaries (*cap*) and veins (*ven*) facing a total resistance that is composed of an arterial and a venous part (R_{art} and R_{ven}). The baroregulation responds to the deviation of the mean arterial pressure (p_{art}) from a reference pressure (p_{ref}), and affects R_{art}, venous unstressed volume ($V_{ven,0}$), heart contractility (E_{max}) and cycle time (T_{cycle}). The Bainbridge reflex responds to the deviation of the mean venous pressure (p_{ven}) from the venous reference pressure ($p_{v,ref}$).The fluid exchange with the environment is determined by a basal fluid intake (J_{intake}), fluid infusion (J_{inf}), bleeding (J_{bleed}), urine production (J_U) and insensible losses (J_{ins}). The fluid exchange between the vascular compartment and the interstitium (*int*) consists of transcapillary fluid flow ($J_{V,TC}$) and lymphatic fluid ($J_{V,L}$). These fluid flows are related to corresponding protein flows, $J_{M,TC}$ and $J_{M,L}$, respectively.

C_{over} and C_{under} determine p_I in hyper-, and hypovolemia, respectively.

Finally, the osmotic pressure is based on the protein concentrations as follows:

$$\pi_{cap} = k_{prot} \cdot c_{PL}, \qquad \pi_I = k_{prot} \cdot c_I, \tag{9}$$

where k_{prot} is an empirical proportionality coefficient.

The lymph flow ($J_{V,L}$), which causes water to be constantly transported back into the intravascular space, depends on the interstitial pressure (Chapple et al., 1993):

$$J_{V,L} = \begin{cases} 0 & p_I < p_{I,ex} \\ J_{L,N} \cdot \left[\frac{p_I - p_{I,ex}}{p_{I,N} - p_{I,ex}}\right] & p_{I,ex} < p_I < p_{I,N} \\ J_{L,N} + LS \cdot (p_I - p_{I,N}) & p_I > p_{I,N} \end{cases}. \tag{10}$$

Here $J_{L,N}$ is the normal lymph flow, $p_{I,ex}$ is the pressure corresponding to the volume $V_{I,ex}$ and LS is the combination of a tissue permeability (L) and surface area (S) in $\frac{\text{ml}}{\text{mmHg}\cdot\text{s}}$.

The elimination of fluids in steady state occurs through insensible losses (J_{ins}), assumed to be constant, and urine production (J_U). J_U is assumed to be linearly related to plasma volume (Gyenge et al., 2003):

$$J_U = \begin{cases} J_{U,N} + k_{UD} \cdot \frac{V_{PL} - V_{PL,N}}{V_{PL,N}} & V_{PL} \leqslant V_{PL,N} \\ J_{U,N} + k_{UE} \cdot \frac{V_{PL} - V_{PL,N}}{V_{PL,N}} & V_{PL} > V_{PL,N} \end{cases}. \tag{11}$$

Here $J_{U,N}$ is the normal urine production at normal plasma volume ($V_{PL,N}$) and $k_{U,D}$ and $k_{U,E}$ govern the change in urine production at depleted and elevated plasma volumes, respectively.

We assume that protein flows (in $\frac{\text{g}}{\text{s}}$) are only associated with the transcapillary protein flow ($J_{M,TC}$), lymph protein flow ($J_{M,L}$) and bleeding ($J_{V,bleed}$). Thus the following mass balances hold:

$$\frac{dM_{PL}}{dt} = -J_{M,TC} + J_{M,L} - J_{V,bleed} \cdot c_{PL} \tag{12}$$

$$\frac{dM_I}{dt} = J_{M,TC} - J_{M,L}, \tag{13}$$

The transcapillary protein flow ($J_{M,TC}$) is based on Kedem and Katchalsky (1958):

$$J_{M,TC} = J_{V,TC} \cdot (1-\sigma) \cdot \left[\frac{c_{PL} - c_{IA}\exp\left(\frac{-J_{V,TC}(1-\sigma)}{PS}\right)}{1 - \exp\left(\frac{-J_{V,TC}(1-\sigma)}{PS}\right)}\right], \tag{14}$$

with $P = \frac{D_M}{h}$, the protein permeability (D_M is the protein diffusion constant, and h is the membrane thickness) and the surface area S, commonly treated as one parameter PS, (protein permeability-surface area product of the capillary).

The lymphatic flow of protein ($J_{M,L}$) is considered to occur through convection only:

$$J_{M,L} = J_L \cdot c_I \tag{15}$$

Finally, to account for bleeding, the following mass balance for red blood cells holds:

$$\frac{dV_{RBC}}{dt} = J_{bleed} \cdot H_{ct}. \tag{16}$$

2.2. Submodel: cardiovascular circulation

To determine the capillary pressure (p_{cap}), used in (7), we implemented a cardiovascular model of the cycle-averaged systemic circulation (Jongen et al., 2016).

The model for the left ventricle is based on Hoppensteadt and Peskin (2002). Cardiac output (J_{CO}) is defined as:

$$J_{CO} = \frac{V_{stroke}}{T_{cycle}}. \tag{17}$$

Here the stroke volume (V_{stroke}) is determined by end diastolic volume (V_{ed}) and end ejection volume (V_{ee}), which in turn depends on the filling (p_{ed}) and ejection pressure (p_{ee}) of the heart. T_{cycle} is cardiac cycle time. We consider a linear pressure-volume relation for diastole and end ejection (Suga et al., 1973):

$$p_{ed} = E_{pas}(V_{ed} - V_{lv,0}); \qquad p_{ee} = E_{max}(V_{ee} - V_{lv,0}) \tag{18}$$

with E_{max} the maximal elastance and E_{pas} the passive elastance of the left ventricle and $V_{lv,0}$ in the left ventricle volume intercept.

For the systemic nodes, the following constitutive equations hold for the mean arterial pressure (p_{art}) and venous pressure (p_{ven}):

$$p_{art} = \frac{V_{art} - V_{art,0}}{C_{art}}; \qquad p_{ven} = \frac{V_{ven} - V_{ven,0}}{C_{ven}}. \tag{19}$$

Here V_{art} is the arterial blood volume, $V_{art,0}$, is the arterial unstressed volume, C_{art} is the arterial compliance, V_{ven} is the venous volume, $V_{ven,0}$ is the unstressed venous volume and C_{ven} is the venous compliance. Since we assume a cycle-averaged system, without pulsatility and valves, we can assume $p_{ee} = p_{art}$ and $p_{ed} = p_{ven}$. Therefore the cardiac output can be calculated as follows:

$$J_{CO} = \frac{1}{T_{cycle}} \cdot \left(\frac{p_{ven}}{E_{pas}} - \frac{p_{art}}{E_{max}}\right). \tag{20}$$

At the same time it holds that:

$$J_{CO} = \frac{p_{art} - p_{ven}}{R_{art} + R_{ven}}, \tag{21}$$

with R_{art} and R_{ven} the arterial and venous capillary resistances in $\frac{\text{mmHg}}{\text{ml}}$, respectively.

Combining (19)–(21) we can determine the arterial and venous pressures analytically:

$$\begin{aligned} p_{art} &= \frac{k_v}{k_a C_v + k_v C_a}(V_{tot} - V_{art,0} - V_{ven,0} - V_{lv,0}); \\ p_{ven} &= p_{art} \cdot \frac{k_a}{k_v}. \end{aligned} \tag{22}$$

with:

$$\begin{aligned} C_a &= C_{art} + \tfrac{1}{2E_{max}}; \qquad C_v = C_{ven} + \tfrac{1}{2E_{pas}}; \\ k_a &= \tfrac{1}{R_{art}} + \tfrac{f_H}{E_{pas}}; \qquad k_v = \tfrac{1}{R_{ven}} + \tfrac{f_H}{E_{max}}, \end{aligned} \tag{23}$$

and

$$f_H = \frac{1}{T_{cycle}}. \tag{24}$$

Finally, the capillary pressure that is used in (7) is calculated by:

$$p_{cap} = p_{ven} + J_{CO} \cdot R_{ven}. \tag{25}$$

2.3. Submodel: cardiovascular regulation

Cardiovascular regulation is modelled by two pathways: baroregulation and the Bainbridge reflex. We model the baroregulation based on Wesseling and Settels (1985) and Jongen et al. (2016). A change in arterial pressure leads to a response of four cardiovascular effectors; the cardiac contractility (E_{max}), cycle time (T_{cycle}), precapillary peripheral resistance (R_{art}) and venous unstressed volume ($V_{ven,0}$). Due to our large timescale, the model has been simplified by neglecting the effector time delays

and low pass filters in the original model. The change in arterial pressure is transformed into a normalised receptor signal $-1 \leqslant b(t) \leqslant 1$, through a sigmoidal receptor function:

$$b(t) = \frac{2}{1 + \exp(-k \cdot (p_{art}(t) - p_{ref}))} - 1, \tag{26}$$

where k controls the sensitivity of the receptor and p_{ref} is the reference mean arterial pressure.

This is translated into the receptor signal (r(t)) after passing through a low pass filter:

$$\frac{dr(t)}{dt} = \frac{1}{\tau_r}(b(t) - r(t)), \tag{27}$$

where τ_r is the low pass filter receptor time constant. The change in E_{max}, R_{art} and $V_{ven,0}$ is calculated by effector specific gains k_E, k_R and k_V:

$$\begin{aligned} E_{max}(t) &= E_{max,0} \cdot (1 + k_E \cdot r(t)); \\ R_{art}(t) &= R_{art,0} \cdot (1 + k_R \cdot r(t)); \\ V_{ven,0}(t) &= V_{ven,0,0} \cdot (1 + k_V \cdot r(t)), \end{aligned} \tag{28}$$

where $E_{max,0}, R_{art,0}$ and $V_{ven,0,0}$ represent the steady state values for the effectors.

The change in T_{cycle} is also affected by the Bainbridge reflex, i.e. the positive chronotropic response of the heart to stretch-activated channels in the atria. In hypervolemia the atria are stretched and this results in extra stimulation of the sino-atrial node, thereby increasing the heart rate. To account for this increase in heart rate we have added a receptor signal (r_a), calculated by a normalised change in venous pressure p_{ven}, with respect to a reference value ($p_{v,ref}$) taken as a substitute for right atrium pressure:

$$r_a(t) = \frac{p_{ven}(t) - p_{v,ref}}{p_{v,ref}}. \tag{29}$$

The cycle time is finally calculated by:

$$T_{cycle}(t) = T_{cycle,0} \cdot (1 + k_T \cdot r(t) + k_{Ta} \cdot r_a(t)). \tag{30}$$

where k_T is the baroregulation effector gain and k_{Ta} is the bainbridge effector gain.

2.4. Parameter estimation

The cardiovascular system was tuned to yield normal steady state hemodynamics for a 70 kg subject, characterised by $p_{art} = 93$ mmHg, $p_{cap} = 11$ mmHg, $p_{ven} = 5$ mmHg, $CO = 5000 \frac{\text{ml}}{\text{min}}$ and $EF = 67\%$.

Most regulation parameters are based on estimations of Wesseling and Settels (1985). For the regulation, p_{ref} is set to normal arterial pressure (93 mmHg) and $p_{v,ref}$ is set to normal venous pressure (5 mmHg). To simulate the response of the model to perturbations we fitted the cardiovascular model output ($\Delta p_{art}, \Delta HR$ and ΔR_{art}) to a dataset from literature (Watenpaugh et al., 1992). In this experimental study the effect of infusion of 30 ml/kg of normal saline, with an infusion rate of 100 ml/min was analysed in seven male volunteers of 78 kg. By manual fitting of k_R and k_{Ta}, the responses of the change in resistance and change in heart rate were tuned to available experimental data. To obtain correct changes in total arterial pressure, the rest of the effect was tuned by fitting k_V.

Settings for many parameters in the fluid exchange model are taken from Xie et al. (1995). Settings for parameters $J_{L,N}, PS$ and J_{intake} were computed to satisfy steady state conditions. Hence, (4), (5), (12) and (14), are assumed to be equal to zero. In normal conditions we assume no intravenous infusion ($J_{inf} = 0$) or bleeding ($J_{bleed} = 0$). Hence, for the sum of the plasma and the interstitial volume it holds that:

$$J_{intake} = J_{ins} + J_{U,N} \tag{31}$$

After setting protein concentrations to values taken from Gyenge et al. (1999), we can determine $J_{L,N}$ and PS analytically, by combining (10) and (14) with:

$$J_{intake} - J_{V,TC} + J_{V,L} - J_U = 0, \tag{32}$$

and:

$$J_{M,TC} - J_{M,L} = 0. \tag{33}$$

The fluid distribution results during infusion ($\Delta V_{PL}, \Delta V_I$ and ΔV_U), were fitted to the experimental results by changing k_f and k_{UE}. All model parameter values are listed in Table 1.

2.5. Simulations

The model was implemented in MATLAB R2014b. Differential equations are solved by an Euler forward integration scheme with a time step of 0.1 s. First, the simulations for parameter estimations as described in Section 2.4 were performed. Secondly, to demonstrate the predictive value of the model on an independent dataset, we simulated an experiment presented by Drobin and Hahn (1999) without additional fitting. There, the authors infused 25 ml/kg in 10 healthy volunteers (with mean bodyweight of 76 kg), being normovolemic or hypovolemic (after induced haemorrhage of 900 ml in 15 min). Experimental and model computed changes of the plasma volume and total urine production at the end of the experiment could be directly compared.

Lastly, we compared our fluid exchange model, with the more complex regulated cardiovascular system, to the fluid exchange model as described in Xie et al. (1995). To this end, we simplified our cardiovascular circulation model to a 'Xie-like' model by replacing E_{max} and E_{pas} by a single elastance value E_{LV}, such that the total compliance of the circulation model was identical to the one used by Xie et al. Due to this simplification we also had to exclude the baroregulation. To solely evaluate the role of the baroreflex, we performed additional simulations with our extended model without baroregulation.

3. Results

3.1. Simulation of the experiment by Watenpaugh et al. (1992)

To reproduce the experimental data, obtained by Watenpaugh et al. (1992), we manually fitted k_f, k_{UE}, k_R, k_V and k_{Ta}, presented in Table 1. Computed results match the experimental results, demonstrating that the model was fitted to the experiment successfully. The changes in volume (per kg body mass), heart rate and arterial pressure in the model and experiment are shown in Fig. 2. During infusion, p_{art} and HR increase with a maximal value of 9 mmHg and 15 bpm, respectively. Maximal p_{ven} is 5.8 mmHg post-infusion. The simulated change in HR can be attributed to a decrease of 10 bpm and increase of 25 bpm, as a result of the baroregulation and Bainbridge reflex. At the end of infusion, the change in plasma and interstitial volume is 11.4 ml/kg and 21.5 ml/kg, respectively. After infusion p_{cap} and p_{art} return towards normal values. However, at 180 min post infusion HR (+3 bpm), and plasma volume (+2.4 ml/kg) are still elevated. Eventually, 14.3 ml/kg urine is produced at the end of the experiment. Interstitial volume decreases more gradually than plasma volume and is still elevated by 11 ml/kg at the end of simulation, which is reflected in an elevated urine production of 11.8 ml/kg compared to a normal production of 2.6 ml/kg.

Table 1
Parameter settings, units and references used for a reference human of 70 kg, with ∗Calculated based on normal hemodynamics as explained in Section 2.4, and subscript 0 indicates the initial value. Parameters k_f, k_{UE}, k_R, k_V and k_{Ta} are fitted on Watenpaugh et al. (1992).

Symbol	Value	Unit	Equation	Reference
C_{art}	2.6	ml/mmHg	(23)	Calculated*
C_{ven}	$2.5 \cdot 10^{2}$	ml/mmHg	(23)	Calculated*
C_{int}	2.0	ml/mmHg	(8)	Xie et al. (1995)
C_{under}	0.6	ml/mmHg	(8)	Xie et al. (1995)
C_{over}	0.1	ml/mmHg	(8)	Xie et al. (1995)
E_{max}	1.7	mmHg/ml	(18)	Calculated*
E_{pas}	$4.4 \cdot 10^{-2}$	mmHg/ml	(18)	Calculated*
$J_{L,N}$	$8.6 \cdot 10^{-3}$	ml/s	(10)	Calculated in steady state
J_{ins}	$1.3 \cdot 10^{-2}$	ml/s	(5)	Watenpaugh et al. (1992)
$J_{U,N}$	$1.7 \cdot 10^{-2}$	ml/s	(11)	Xie et al. (1995)
k_f	0.2	ml/mmHg·s	(7)	Fitted on Watenpaugh et al. (1992)
k_{prot}	0.4	mmHg · ml/g	(9)	Gyenge et al. (2003)
k_{UE}	$3.5 \cdot 10^{-4}$	ml/s	(11)	Gyenge et al. (2003)
k_{UD}	$4.6 \cdot 10^{-5}$	ml/s	(11)	Gyenge et al. (2003)
k	$7.5 \cdot 10^{-2}$	1/mmHg	(26)	Wesseling and Settels (1985)
k_T	0.6	-	(30)	Wesseling and Settels (1985)
k_{Ta}	−2.2	-	(30)	Fitted on Watenpaugh et al. (1992)
k_E	−0.2	-	(28)	Wesseling and Settels (1985)
k_R	−0.7	-	(28)	Fitted on Watenpaugh et al. (1992)
k_V	0.9	-	(28)	Fitted on Watenpaugh et al. (1992)
LS	$1.2 \cdot 10^{-2}$	ml/mmHg · s	(10)	Xie et al. (1995)
PS	$6.9 \cdot 10^{-3}$	ml/s	(14)	Calculated in steady state
$p_{I,ex}$	−0.1	mmHg	(10)	Xie et al. (1995)
$p_{I,N}$	−0.7	mmHg	(8), (10)	Xie et al. (1995)
$p_{I,over}$	1.8	mmHg	(8)	Xie et al. (1995)
p_{ref}	93	mmHg	(26)	Normal hemodynamics
$p_{v,ref}$	5.0	mmHg	(29)	Normal hemodynamics
$M_{PL,0}$	224.0	g	(2)	Xie et al. (1995)
$M_{I,0}$	250.3	g	(3)	Xie et al. (1995)
R_{art}	908.0	mmHg s/ml	(23)	Calculated*
R_{ven}	62.7	mmHg s/ml	(23)	Calculated*
τ_r	1.0	s	(27)	Wesseling and Settels (1985)
T_{cycle}	0.8	s	(17), (20), (24), (30)	Normal hemodynamics
$V_{art,0}$	746.6	ml	(22)	Calculated*
$V_{I,N}$	8400	ml	(3), (8)	Xie et al. (1995)
$V_{I,EX}$	2100	ml	(3)	Xie et al. (1995)
$V_{Iv,0}$	0	ml	(22)	Normal hemodynamics
$V_{ven,0}$	2433	ml	(22)	Calculated*
$V_{PL,N}$	3200	ml	(1), (11)	Xie et al. (1995)
$V_{RBC,0}$	1800	ml	(1)	Xie et al. (1995)
σ	0.99	-	(7), (14)	Xie et al. (1995)

3.2. Simulation of the experiment by Drobin et al. (1999)

In Fig. 3, the simulated and experimental (Drobin and Hahn, 1999) changes in volume distribution in hypo- and normovolemia are shown. As in the experiment, changes are reported with respect to the start of infusion, set at t = 0 for both scenarios. In the normovolemic simulation, infusion causes a maximal change in plasma volume of 8.4 ml/kg, which corresponds to the measured plasma dilution. For hypovolemia the change in plasma volume (+10.3 ml/kg) also corresponds to the experimental results. The differences in p_{cap} show the effect of pre-infusion haemorrhage. The difference between hypo- and normovolemia results is most pronounced in the simulated urine production. Cumulative urine production at 180 min post infusion is reported to be 12.3 ± 1 ml/kg and 9.7 ± 2 ml in normo-, and hypovolemia, respectively. The model captures this in the normovolemic case (11.4 ml/kg), but not in the hypovolemic case (3.6 ml/kg). This results in an elevated interstitial volume in the latter case.

3.3. Comparison to the 'Xie-like' model

To further evaluate our extended model, we also simulated the Watenpaugh experiment with our reduced 'Xie-like' model, that resembles the model by Xie et al. (1995), as shown in Fig. 2. The 'Xie-like' model does not include p_{art} and HR. As compared to our extended model, it does predict an increased maximum rise in p_{cap} (15.1 vs. 13.1 mmHg). Consequently, more fluid is transported from the plasma into the interstitium and urine production is reduced at the end of the experiment by 2 ml/kg.

Finally, the effect of regulation was evaluated by simulating the Watenpaugh experiment without baroregulation (Fig. 2). This results in an increased p_{art} (38 mmHg vs. 9 mmHg post infusion) and no changes in HR. Results for changes in capillary pressure, plasma and interstitial volume, and urine production are similar to those of the 'Xie-like' model.

4. Discussion

Optimisation of perioperative fluid administration remains difficult due to high patient variability and the lack of tools to directly measure patient fluid status. Mathematical models have the potential of improving fluid administration protocols. Previously developed mathematical models focussed on describing the fluid exchange over time but they lacked clinically measurable indices such as heart rate and arterial blood pressure. The aim of our study was to make a first step towards a clinically applicable fluid

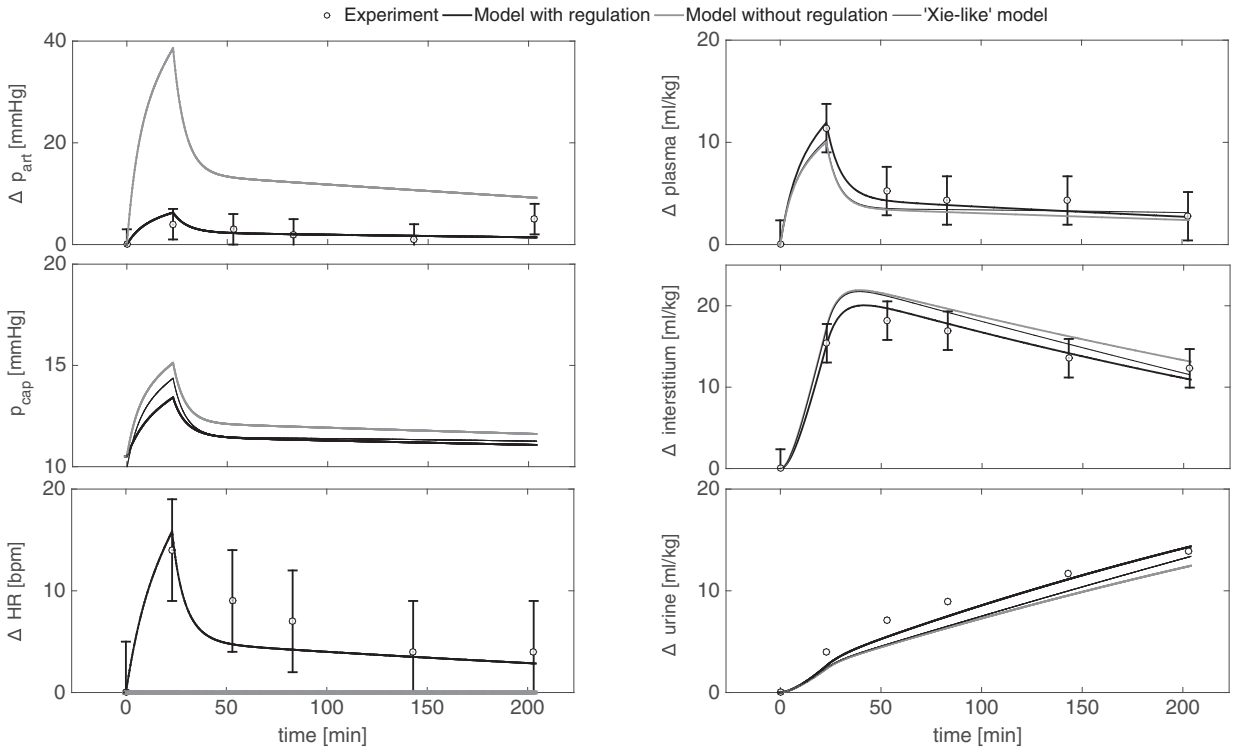

Fig. 2. Simulation of the experiment of Watenpaugh et al. (1992), with 30 ml/kg saline infusion from t = 0 to t = 23 min; experimental results are shown in symbols; simulation results are shown in solid lines, for the model with regulation, without regulation and the 'Xie-like' model. Left: change in mean arterial pressure (Δp_{art} in mmHg), absolute capillary pressure (p_{cap} in mmHg) and change in heart rate (ΔHR in bpm). Right: scaled changes in plasma (ΔV_{PL} in $\frac{\text{ml}}{\text{kg}}$), interstitial ($\Delta V_I$ in $\frac{\text{ml}}{\text{kg}}$) and urine volume ($\Delta V_U$ in $\frac{\text{ml}}{\text{kg}}$).

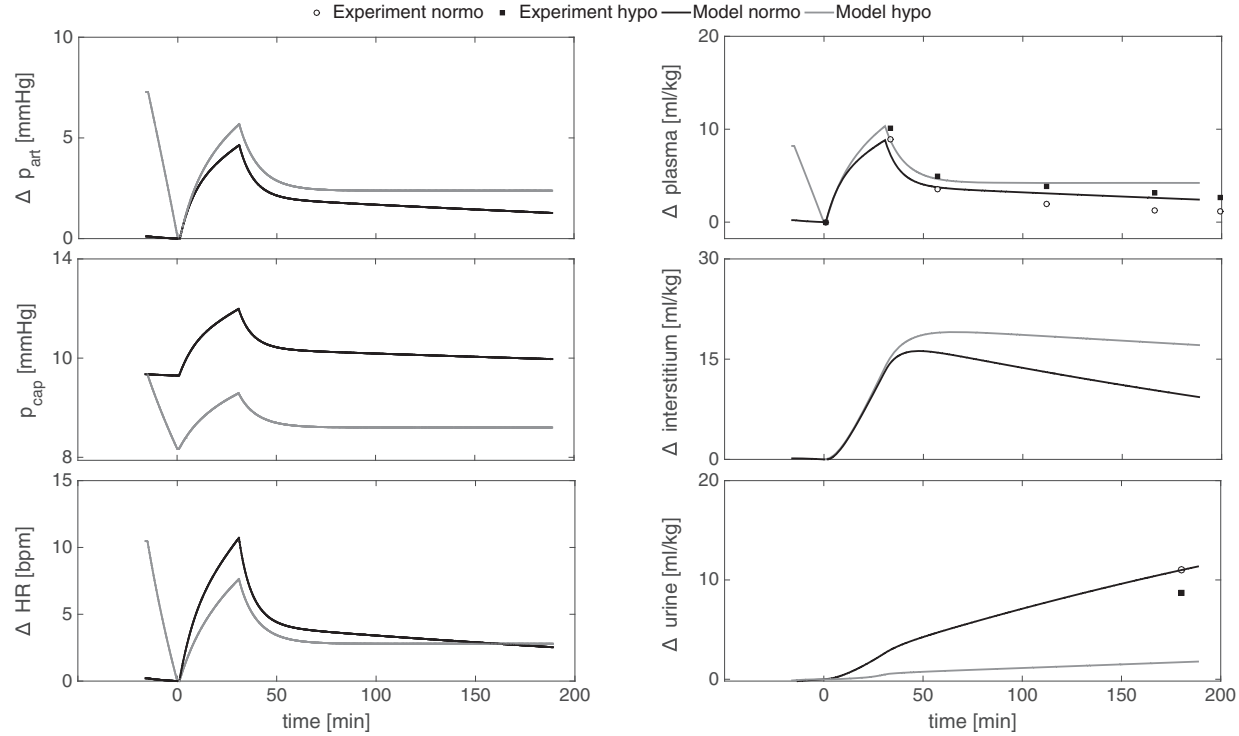

Fig. 3. Simulation of the experiment by Drobin et al. (1999); results of 25 ml/kg saline infusion in a normovolemic and hypovolemic state. Left: the change in mean arterial pressure (Δp_{art} in mmHg), absolute capillary pressure (p_{cap} in mmHg), change in heart rate (ΔHR in bpm). Right: scaled changes in plasma (ΔV_{PL} in $\frac{\text{ml}}{\text{kg}}$), interstitial ($\Delta V_I$ in $\frac{\text{ml}}{\text{kg}}$) and urine volume ($\Delta V_U$ in $\frac{\text{ml}}{\text{kg}}$). Experimental data (from Drobin et al. (1999)) are shown with symbols.

administration support model, by combining existing fluid exchange models (Xie et al., 1995; Gyenge et al., 2003) with a cardiovascular circulation model that includes baroregulation (Jongen et al., 2016) and the Bainbridge reflex. To the best of our knowledge this is the first time that such a coupling of short- and long term effects (cardiovascular regulation and fluid exchange, respectively) has been made.

Our model was used to study the effects of fluid infusion and blood loss in healthy volunteers. We could fit the model to predict the fluid exchange in one experiment (Watenpaugh et al., 1992) and subsequently reproduce results from another experiment (Drobin and Hahn, 1999) without further tuning. The Watenpaugh experiment was also simulated in our model without regulation, and in a 'Xie-like' model. Here, the increase in interstitial volume is approximately 10% lower in the extended model. We conclude that differences between our extended model and the 'Xie-like' model are mainly due to the addition of the (short term) regulation.

To achieve our goal of clinical decision support, the right balance between model complexity and accuracy must be made. The current goal was to study long term effects of fluid infusion on volume distribution in volunteers and their hemodynamic response in terms of mean arterial pressure and heart rate. Therefore, we chose to use a model for cycle-averaged hemodynamics without beat-to-beat information, which reduces the amount of parameters that needs to be estimated. We implemented the traditional Starling Eq. (7) to model whole-body transcapillary transport. Experiments (Michel and Philips, 1987) have shown that there is a distinction between transport in normal capillaries, where reabsorption of fluid seems absent, and fenestrated capillaries, where reabsorption is present. In recent years there has been an adaptation of the Starling equation, to better capture fluid exchange in capillaries (Adamson et al., 2004). However, we adopted the traditional Starling approach, since in our lumped parameter approach spatial variations, and hence variations in capillary type, are not taken into account. Lastly, we assumed urine production solely based on plasma volume, thereby omitting the effects of hormone regulation pathways such as the RAAS mechanism.

The three fitted parameters in the fluid exchange model (k_f, $J_{L,N}$ and PS) can be compared to previously presented values (Gyenge et al., 1999; Tatara et al., 2007). k_f is the determining factor for the maximum plasma expansion during infusion, and determines the persisting level after infusion. Our fitted value is 0.15 $\frac{\text{ml}}{\text{mmHg}\cdot\text{s}}$, which is high compared to 0.03 $\frac{\text{ml}}{\text{mmHg}\cdot\text{s}}$, reported in Gyenge et al., and 0.08 $\frac{\text{ml}}{\text{mmHg}\cdot\text{s}}$ in Tatara et al. (2007). But it is still within the range reported in literature (0.008–0.34 $\frac{\text{ml}}{\text{mmHg}\cdot\text{s}}$, Chapple et al. (1993)). PS and $J_{L,N}$ were derived from the condition of homeostatic equilibrium, i.e. from the condition of equal fluid intake and loss over time. Our calculated value for $J_{L,N}$ (0.009 $\frac{\text{ml}}{\text{s}}$) is low compared to literature values (0.02–0.04 $\frac{\text{ml}}{\text{s}}$, Reddy, 1986). PS is hard to estimate from literature, however this parameter is closely correlated to the estimation of σ ($0.8 - 0.99$ [–], Chapple et al., 1993). Ultimately, the transcapillary transport is not characterised by the individual values of these parameters, but by their combination (14), as expressed by the Péclet number: $Pe = (1-\sigma)J_{V,TC}/PS$. Comparing our results ($\sigma = 0.99, Pe = 0.0106$) to Gyenge ($\sigma = 0.99, Pe = 0.0103$) and Tatara et al. (2007) ($\sigma = 0.875, Pe = 0.046$), shows the same order of magnitude. Thus, the Péclet number and therefore the combination of σ and PS is supported by literature.

Cardiovascular regulation is described by baroregulation and the Bainbridge reflex. In this study the venous pressure ($p_{v,ref}$) is taken as a substitute for atrial pressure. This simplification is inherent to our choice of a simplified heart model. The change in HR by +15 bpm due to an increase of $p_{v,ref}$ by 1 mmHg, predicted by the model is supported by literature. Experimental data reported in Kohl et al. (1999) show an increase in the same order of magnitude (+8 bpm).

The predictive value of the model is demonstrated, since results of Drobin and Hahn (1999) are captured quite well with the same fitted parameters. Notably, there is an underestimation of urine production in the hypovolemic simulation (3.6 ml/kg vs 9.7 ml/kg). The urine production during hypovolemia is governed by parameter k_{UD} in (11), adopted from Gyenge et al. (2003), since this could not by fitted from the Watenpaugh dataset. Fitting of k_{UD} to the Drobin dataset proved to be impossible due to the fact that $J_{U,N}$ is four times smaller than the experimental J_U. However, in other studies (Gupta and Gan, 2016) a hypovolemic urine production of 1.5 ml/kg was reported, demonstrating considerable variation in between experimental data.

Our final goal is to develop a decision support model that can eventually assist in fluid administration to critically ill patients. It is known that fluid exchange in the perioperative period is altered. Perioperative medication for anaesthesia, analgesia and hemodynamic support affect (baro) regulation and renal function, which influences capillary fluid exchange. Additionally there can be effects of surgical inflammation causing capillary leakage (Brandstrup, 2006). In our model this can be accounted for in parameters related to membrane permeability (e.g. σ and k_f in 7).

Moreover, patients may suffer from comorbidities such as cardiac dysfunction, renal insufficiency and chronic hypertension. Therefore, in future work we need to extend the cardiac and renal model, to allow for realistic simulation of these pathologies.

For eventual use in a specific patient, suitable parameter values have to be found using data assimilation techniques. To gain more insight into the possibilities for parameter fixing and prioritisation, a structured sensitivity analysis (Eck et al., 2016) should also be performed. Additionally this could indicate which submodels should be explored further.

To conclude, we combined a simple model for cardiovascular hemodynamics with an existing model for fluid exchange for healthy volunteers enabling coupling of readily available clinical measurements to a fluid exchange model. This is the first step towards our general aim to develop a patient-specific decision support model to guide fluid administration.

Conflict of interest

Dr. R. Arthur Bouwman declares to be part-time employed at Philips Research Eindhoven. No further conflicts of interest are declared by the authors.

Acknowledgement

This work was performed within the IMPULS II perioperative monitoring framework in collaboration with Philips Eindhoven.

References

Adamson, R.H., Lenz, J.F., Zhang, X., Adamson, G.N., Weinbaum, S., Curry, F.E., 2004. Oncotic pressures opposing filtration across non-fenestrated rat microvessels. J. Physiol. 557, 889–907.

Brandstrup, B., 2006. Fluid therapy for the surgical patient. Best Pract. Res. Clin. Anaesthesiol. 20, 265–283.

Carlson, D.E., Kligman, M.D., Gann, D.S., 1996. Impairment of blood volume restitution after large hemorrhage: a mathematical model. Am. J. Physiol. 270, R1163–R1177.

Chapple, C., Bowen, B.D., Reed, R.K., Xie, S.L., Bert, J.L., 1993. A model of human microvascular exchange: parameter estimation based on normals and nephrotics. Comput. Methods Programs Biomed. 41, 33–54.

Drobin, D., Hahn, R.G., 1999. Volume kinetics of Ringer's solution in hypovolemic volunteers. Anesthesiol.: J. Am. Soc. Anesthesiol. 90, 81–91.
Eck, V.G., Donders, W.P., Sturdy, J., Feinberg, J., Delhaas, T., Hellevik, L.R., Huberts, W., 2016. A guide to uncertainty quantification and sensitivity analysis for cardiovascular applications. Int. J. Numer. Meth. Biomed. Eng. 32, e02755.
Gupta, R., Gan, T.J., 2016. Peri-operative fluid management to enhance recovery. Anaesthesia 71, 40–45.
Gyenge, C.C., Bowen, B.D., Reed, R.K., Bert, J.L., 1999. Transport of fluid and solutes in the body I. Formulation of a mathematical model. Am. J. Physiol.-Heart Circul. Physiol. 277, H1215–H1227.
Gyenge, C.C., Bowen, B.D., Reed, R.K., Bert, J.L., 2003. Mathematical model of renal elimination of fluid and small ions during hyper- and hypovolemic conditions. Acta Anaesthesiol. Scand. 47, 122–137.
Hahn, R.G., 2010. Volume kinetics for infusion fluids. Anesthesiology 113, 470–481.
Hahn, R.G., 2017. Arterial pressure and the rate of elimination of crystalloid fluid. Anesth. Analg. 124, 1824–1833.
Hahn, R.G., Svensén, C., 1997. Plasma dilution and the rate of infusion of Ringer's solution. Br. J. Anaesth. 79, 64–67.
Holte, K., Sharrock, N., Kehlet, H., 2002. Pathophysiology and clinical implications of perioperative fluid excess. Br. J. Anaesth. 89, 622–632.
Hoppensteadt, F., Peskin, C., 2002. Modeling and Simulation in Medicine and Life Sciences. Springer-Verlag, New York.
Jongen, G.J., van der Hout-van der Jagt, M.B., van de Vosse, F.N., Oei, S.G., Bovendeerd, P.H., 2016. A mathematical model to simulate the cardiotocogram during labor. Part A: Model setup and simulation of late decelerations. J. Biomech. 49, 2466–2473.
Kedem, O., Katchalsky, A., 1958. Thermodynamic analysis of the permeability of biological membranes to non-electrolytes. Biochim. Biophys. Acta 27, 229–246.
Kohl, P., Hunter, P., Noble, D., 1999. Stretch-induced changes in heart rate and rhythm: clinical observations, experiments and mathematical models. Prog. Biophys. Mol. Biol. 71, 91–138.
Mazzoni, M.C., Borgström, P., Arfors, K.E., Intaglietta, M., 1988. Dynamic fluid redistribution in hyperosmotic resuscitation of hypovolemic hemorrhage. Am. J. Physiol. 255, H629–H637.
Michel, C.C., Philips, M.E., 1987. Steady state fluid filtration at different capillary pressures in perfused frog mesenteric capillaries. J. Physiol. 388, 421–435.
Reddy, N., 1986. Lymph circulation: physiology, pharmacology, and biomechanics. Crit. Rev. Biomed. Eng. 14, 45–91.
Suga, H., Sagawa, K., Shoukas, A.A., 1973. Load independence of the instantaneous pressure-volume ratio of the canine left ventricle and effects of epinephrine and heart rate on the ratio. Circ. Res. 32, 314–322.
Svensén, C., Ponzer, S., Hahn, R.G., 1999. Volume kinetics of Ringer solution after surgery for hip fracture. Can. J. Anesth. 46, 133.
Tatara, T., Tsunetoh, T., Tashiro, C., 2007. Crystalloid infusion rate during fluid resuscitation from acute haemorrhage. Br. J. Anaesth. 99, 212–217.
Watenpaugh, D.E., Yancy, C.W., Buckey, J.C., Lane, L.D., Hargens, A.R., Blomqvist, C. G., 1992. Role of atrial natriuretic peptide in systemic responses to acute isotonic volume expansion. J. Appl. Physiol. 73, 1218–1226.
Wesseling, K., Settels, J., 1985. Baromodulation explains short-term blood pressure variability. In: Psychophysiology of Cardiovascular Control: Models, Methods and Data. Plenum Press, New York, pp. 69–97.
Wolf, M., Deland, E., 2011. A mathematical model of blood-interstitial acid-base balance: application to dilution acidosis and acid-base status. J. Appl. Physiol. 110, 988–1002.
Wolf, M., Watson, P., 1989. Measurement of osmotic reflection coefficient for small molecules in cat hindlimbs. Am. J. Physiol. - Heart Circul. Physiol. 256, H282–H290.
Wolf, M.B., 2013. Whole body acid-base and fluid-electrolyte balance: a mathematical model. Am. J. Physiol. Renal Physiol. 305, F1118–31.
Xie, S., Reed, R., Bowen, B., Bert, J., 1995. A model of human microvascular exchange. Microvasc. Res. 49, 141–162.